Design of Cocrystals for Molecules with Limited Hydrogen Bonding Functionalities: Propyphenazone as a Model System

Lucy K. Mapp,[†,‡] Simon J. Coles,[‡] Srinivasulu Aitipamula*[,†]

[†] *Crystallization and Particle Science, Institute of Chemical and Engineering Sciences, A*STAR (Agency for Science, Technology and Research), 1 Pesek Road, Jurong Island, 627833, Singapore.*

[‡]*Chemistry, Faculty of Natural and Environmental Sciences, University of Southampton, University Road, Southampton, SO17 1BJ, UK.*

KEYWORDS

Cocrystal, Crystal Engineering, Design, Hydrogen Bonding, Interactions, Pharmaceutical, Properties

ABSTRACT:

We report eight new cocrystals with an analgesic drug, propyphenazone, which belongs to a family of compounds that possess limited or no hydrogen bonding functionality. Such molecules

present difficulties in predicting and selecting appropriate coformers for potential multicomponent systems, and current prediction methodologies are unsuitable due to their focus around hydrogen bonding. This study used a knowledge-based strategy to identify appropriate coformers as well as testing a wide variety of molecules to confirm the initial predictions. All new cocrystals were characterized using X-ray diffraction techniques as well as measuring their physiochemical properties. These included the thermal behavior, stability under slurry and accelerated conditions, solubility and dissolution rate and were compared with the parent propyphenazone. It was found that while the stability of most of the cocrystals and propyphenazone was comparable, a cocrystal with hydroquinone showed an increase in both the solubility and dissolution rate of propyphenazone.

INTRODUCTION

Cocrystals[1-3] are well established in the literature as a route to new and alternative solid forms, and a promising method for fine-tuning properties[4, 5] of a molecule. Pharmaceutical cocrystals[5-9] are cocrystals that consist of an active pharmaceutical ingredient (API) and a pharmaceutically acceptable coformer that is a solid under ambient conditions. Recent case studies in the literature have demonstrated diverse applications of cocrystals in modifying physicochemical properties whilst retaining the biological activity and structure of the API (unlike in a salt form). By judicious selection of coformers[10] one can fine-tune the properties such as solubility, dissolution rate, stability, bioavailability, mechanical strength, permeability, etc.[11-14]

Design of cocrystals *a priori* is desirable to focus experimental work and reduce the number of trials required to achieve the desired result. Wood *et al*[15] have summarised the rational design

strategies from the past and highlighted future directions of this field. A crystal engineering or supramolecular synthon-based approach,[16-19] is a convenient and common method used in the design of such systems, implementing frequently occurring motifs from literature applicable to the functional groups present in the API of interest. This method is established from the work by Etter[20, 21] and the proposed rules for organic compounds which were defined based upon the predictability of hydrogen bonds. A supramolecular synthon approach fails, however, when no such groups are present in the molecular structure. When functional groups are limited, e.g. no donors or minimal acceptors are present, finding reliable synthons is also difficult. Hence, the subsequent design poses a greater challenge. Examples of some APIs that are devoid of such donor functionalities include griseofulvin,[22] spironolactone[23] and artemisinin[24] which produced limited success from extensive cocrystal screens. In these studies, both griseofulvin and spironolactone produced just one cocrystal product, whilst artemisinin formed two. Coformer selection for these systems was based primarily upon trial and error, as no methodology is clearly defined, although some knowledge was introduced into the artemisinin study.

Laszlo Fábián[25] reported an alternative prediction methodology based on molecular complementarity. This method used quantitative structure activity relationship (QSAR) based descriptors to describe each molecule in the cocrystal and presented some boundary conditions indicating sufficient similarity in parent and coformer structure for a cocrystal to be likely to form. The model is based primarily upon shape and polarity descriptors and was implemented in the cocrystal prediction study on artemisinin by Jones and co-workers.[24] The prediction calculations indicated 41 of the 75 coformers used in the study would result in cocrystal formation. However, despite a thorough cocrystal screening by solid-state grinding techniques,

only two cocrystals were produced experimentally. This indicates that the molecular descriptor-based method is, as yet, perhaps not best suited to cocrystal design for such molecules.

An alternative prediction method (to those aforementioned and described in the literature) is to use a knowledge-based approach interrogating the wealth of knowledge encompassed within the crystal structures deposited in the Cambridge Structural Database (CSD),[26] along with the various software components provided by the Cambridge Crystallographic Data Centre (CCDC). These allow interaction and fragment searching in Isostar[27] and Conquest[28] as well as full interaction mapping and contact searching with specific interaction motifs in Mercury.[29, 30] Many of these software programs allow the environment to be easily varied and manipulated, with the inclusion and modification of restraints, to best describe the chemical space of interest. Hence, it is possible to see how certain changes can affect the interaction or behaviour of a functional group.

Propyphenazone (1,5-Dimethyl-2-phenyl-4-propan-2-yl-pyrazol-3-one, PROPY) is an API with antipyretic and analgesic effects which has been marketed as a component of the combination drug, Saridon,[31] used as a painkiller. This falls into the aforementioned class of drug molecules lacking hydrogen bonding donor groups and containing only one acceptor atom. In addition, the presence of an isopropyl group next to the carbonyl group leads to a degree of steric hindrance by limiting the geometric possibilities for intermolecular interactions to form (Figure 1). Herein, we take this molecule as a case study to apply knowledge-based prediction methodology to find potential coformers for synthesis of new cocrystals.

RESULTS AND DISCUSSION

Three polymorphs of PROPY have been reported by Müller and Beer in 1982[32] with melting points of 104.3 °C, 102.5 °C and 101 °C for forms I, II and III respectively. Form II is the stable form at room temperature with I and III being metastable, the latter only occurring with the other forms rather in isolation.[33, 34] Both Forms I and III convert to Form II on storage and heating (Form I) and very quickly during handling (Form III). Crystal structures of Forms I (*Pc*) and II (*Cc*) obtained from X-ray powder diffraction data have been reported recently by Lemmerer *et al.*[33] Forms I and II are very similar in their cell parameters and in the primary intermolecular interaction (C–H···O), which occurs between the methyl substituent adjacent to the isopropyl group and carbonyl of an adjacent molecule. Lemmerer *et al.* have also reported a drug-drug cocrystal[33, 35] involving PROPY interacting with pyrithyldione through a single N–H···O (carbonyl) hydrogen bond. This indicates the potential to form cocrystals with PROPY and make it a realistic and appropriate probe for a study focussing on an API with limited hydrogen bonding functionalities.

Interaction Searching. The CSD data was interrogated to identify the potential interactions that could occur for PROPY and thereby aid in the selection of likely coformers for subsequent cocrystal screening. An Isostar[27] search identified that aromatic amines, aliphatic hydroxyls or carboxylic acids, followed by aromatic hydroxyls return the greatest number of structures forming an interaction with a carbonyl group (see Supporting Information 1.1). Interaction analysis utilising Mercury's[29] motif searching for specific contacts allows for greater flexibility and specificity in the description of the donor groups/fragments. A number of different models with differing chemical environments for the carbonyl group were used to achieve a balance of describing the chemical environment and neighbouring atoms to reflect the carbonyl in PROPY,

whilst also ensuring sufficient hits were returned to allow reliable conclusions to be drawn. The most representative model for the carbonyl group in the PROPY (a pyrazolone ring) returned limited results with few structures to learn from. Subsequent fragment searches were therefore made more general by applying fewer restraints (see Supporting Information, section 1.2). A wide variety of donor groups and descriptions (kept constant in all searches) were used in order to provide a more detailed understanding of not only the functional groups but also their chemical environment. In general from this analysis, NH_2, OH and CO_2H functionalities were found to be the most suited donor groups for this system, and therefore coformers containing such functional groups were chosen to drive the cocrystal screening process.

The case study compound, PROPY, shows structural similarity to two other compounds, antipyrine and edaravone, which contain the same molecular skeleton (phenylpyrazole) however PROPY contains an isopropyl ring substituent which causes steric hindrance at the carbonyl (Figure 1). A number of multicomponent systems[36-43] have been reported for antipyrine and edaravone, from which additional knowledge can be gained and can be used in the design and search for cocrystals of PROPY. An analysis of these systems indicate that most of the coformers feature CO_2H donor groups. Additionally, structural analysis of the antipyrene cocrystals revealed that the main interactions of the carbonyl group involves predominantly NH_2 or CO_2H donor groups. This structural analysis reinforces our interaction search results with PROPY and further aids in coformer selection.

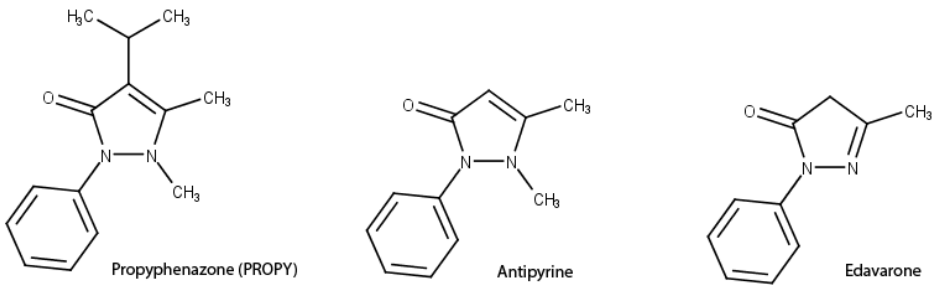

Figure 1. Molecular structures of propyphenazone, antipyrine, and edaravone.

Coformer Selection and Screening. A selection of coformers containing the main functional groups identified in the CSD examinations, either in isolation or in various combinations, were selected for screening experiments. Some coformers either totally lacking in the identified functional groups, or including alternative ones, were also included to act as a control and therefore investigate the suitability of these knowledge-based predictions (see Supporting Information, section 2.1). Solvent drop and neat grinding methods[44-46] were applied to the selected parent-coformer combinations.

Grinding experiments on a number of combinations produced powders for which the PXRD patterns are different from those of the parent materials. These included six coformers for which single crystals were obtained (*vide infra)*, as well as a number of samples for which no single crystals have yet been produced (see Supporting Information, sections 3.1 and 3.2).

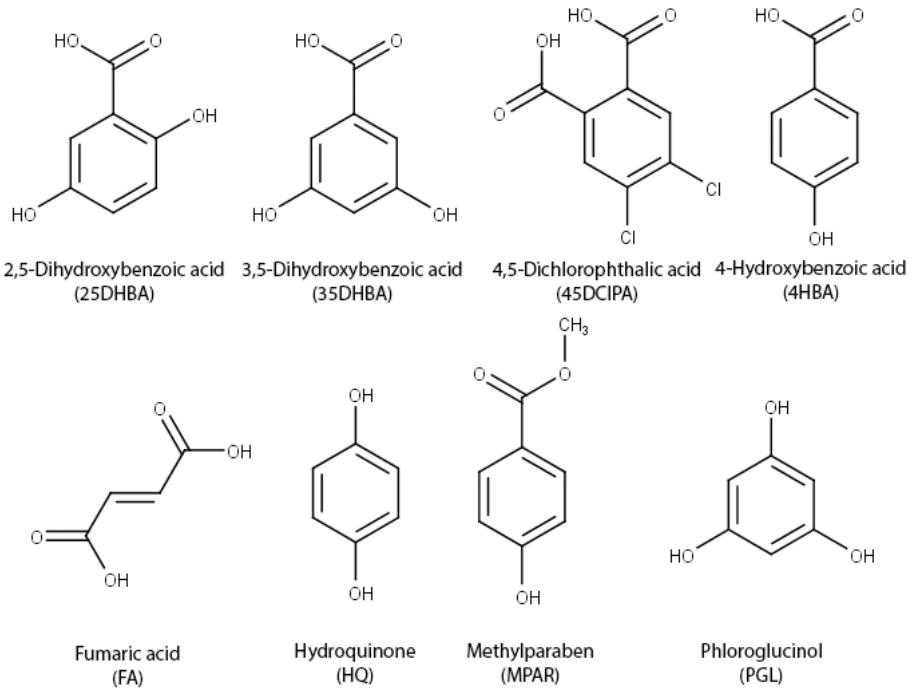

Figure 2. Molecular structures of coformers which produced cocrystals with PROPY.

Screening by grinding methods presented difficulties in some instances due to the low melting point of PROPY (~100 °C) causing a number of combinations to produce a sticky paste, gel or liquid in the grinding jar which could not be characterised by PXRD. Subsequent dry (neat) and manual grinding approaches for many of these combinations also resulted in pastes and liquids and so the characterisation was not viable (see Supporting Information, section 3.3). Many of these compounds have similar chemical structures to the coformers in our successful pairings and therefore it would be reasonable to expect that cocrystals may form under different conditions. Solution crystallisation experiments were attempted for some of these combinations

and two coformers, 2,5-dihydroxybenzoic acid and its 3,5-disubstituted analogue, produced single crystals suitable for characterisation and subsequent analysis.

Molecular Complementarity (QSAR) Prediction. The prediction methodology of Fábián was applied to a selection of coformers and PROPY in order to compare to experimental findings (both positive and negative). The CSD-Materials suite in Mercury (v3.8, build RC2) was used to generate descriptor values and to determine whether pairing with PROPY was likely to give a cocrystal. The pre-loaded set of coformers was utilised and supplemented with experimentally discovered results using 3D geometry optimised MOL files generated from drawn structures using the MarvinSketch software.[47]

Experimental results and predictions are provided as Supporting Information (section 2.2) from which it can be seen that the prediction model is not best suited to this class of compounds i.e. those with minimal, or no, hydrogen bonding functionalities. The eight coformers that formed cocrystals fall into both the pass and fail lists in an almost equal distribution. Similarly combinations from screening by grinding that indicated potential for a new form and those which showed no changes when compared to the parent reference materials, are spread across both groups of predictions.

Crystal Structures. Full details of structural parameters and descriptions are provided in the Supporting Information, section 4. Of the eight cocrystals synthesised in this study, two (phloroglucinol and 2,5-dihydroxybenzoic acid) form solvates in 1:1:0.5 and 2:1:1 ratios respectively. All but two form in a 1:1 ratio, with the exceptions being hydroquinone (1:2 stoichiometric ratio) and fumaric acid (1:0.5 ratio).

The structures can be classified into three groups according to their functional groups and interactions (Figure 2):

- coformers containing only hydroxyl donor functionalities and forming a hydroxyl···carbonyl hydrogen bond
- coformers containing only carboxylic acid donor functionalities and forming an acid···carbonyl hydrogen bond
- coformers which possess both hydroxyl and carboxylic acid functional groups, yet display hydroxyl···carbonyl hydrogen bonds.

Hydroxyl Functional Group. Three cocrystals were obtained with coformers containing only OH functional groups: methylparaben (MPAR), phloroglucinol (PGL) and hydroquinone (HQ).

PROPY-MPAR (1:1) cocrystal. The assembly of this 1:1 complex is primarily based on a bifurcated carbonyl hydrogen bonding pattern, consisting of an O–H···O (D···A distance 2.63 Å, D–H···A angle 174°) hydrogen bond and a C–H···O (3.19 Å, 126°) interaction from coformer to PROPY carbonyl (Figure 3), which generate a puckered hydrogen bonded chain. These chains occur in two orientations, each stacking into layers which run approximately along and parallel to the (1 0 0) plane respectively. When viewed down the *b*-axis these can be seen as double layers propagating in the *a*-axis direction.

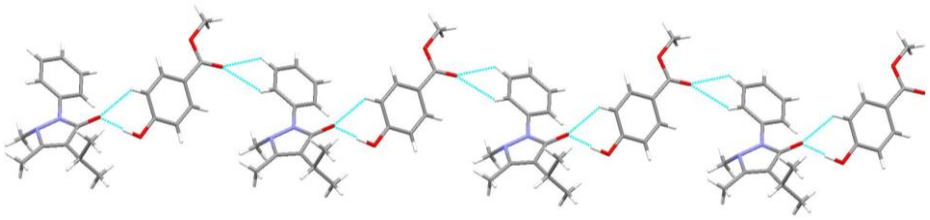

Figure 3. Crystal structure of PROPY-MPAR cocrystal displaying the main hydrogen bonding chain.

PROPY–PGL acetonitrile (2:2:1) solvate. The asymmetric unit of the cocrystal contains two molecules of each of the coformer and API, along with one additional acetonitrile solvent molecule. The primary interaction between coformer and PROPY is an O–H···$O_{carbonyl}$ (2.63 Å and 2.749 Å, both 169°) hydrogen bond which forms a bifurcated interaction to the carbonyl with a second, similar hydrogen bond (2.63 Å and 2.66 Å, 168° and 176°). The two molecules of PGL are not equivalent, as one partakes in three O–H···O hydrogen bonds to PROPY and the other forms one O–H···$O_{carbonyl}$ to PROPY, one O–H···$O_{hydroxyl}$ to the first PGL and an O–H···N hydrogen bond to the solvent molecule. These interactions form a chain containing central PGL molecules which extend into sheets via the bifurcated carbonyl hydrogen bonds of the second PROPY molecule. The sheets stack in layers with alternating orientations as shown in the right of Figure 4.

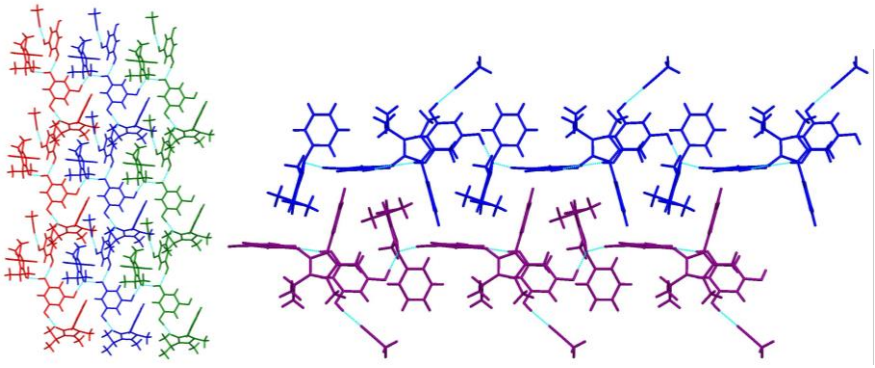

Figure 4. PROPY-PGL cocrystal chains forming sheets (left) which stack into layers (right) where a single coloured layer (blue or purple) represents the red-blue-green sheet on the left.

PROPY–HQ (1:2) cocrystal. PROPY forms a 1:2 complex with HQ through O–H···O hydrogen bonds (2.69 Å and 2.57 Å, 172° and 175°), resulting in HQ molecules that are arranged approximately perpendicular to one another. Hydrogen bonds between the HQ molecules extend these 2:1 units into double layer corrugated chains (Figure 5). These chains propagate throughout the structure to give double layers running perpendicular to the *a*-axis.

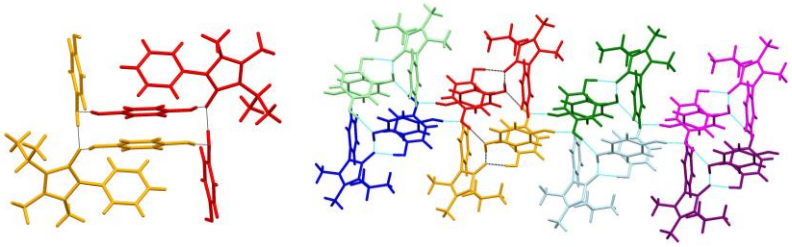

Figure 5. Double chain structure viewed down the chain (left) and side-on, coloured by 2:1 units (right) in the crystal structure of PROPY-HQ cocrystal.

Carboxylic Acid Functional Group. Two cocrystals were obtained with coformers containing only a carboxylic acid functional group in the molecule. These were fumaric acid (FA) and 4,5-dichlorophthalic acid (45DClPA).

PROPY–FA (1:0.5) cocrystal. The asymmetric unit of the cocrystal contains a PROPY molecule and half a molecule of FA which form a single, linear carboxylic acid O–H···$O_{carbonyl}$ hydrogen bond (2.57 Å, 170°). The FA lies on an inversion centre, which gives rise to a 1:0.5 API-coformer stoichiometry (Figure 6). These units form a number of C–H···O contacts which result in a stepped motif where the PROPY phenyl rings are arranged in an offset face-to-face configuration with respect to each other. These stepped chains pack into layers along the *a*-axis to give the three-dimensional crystal structure.

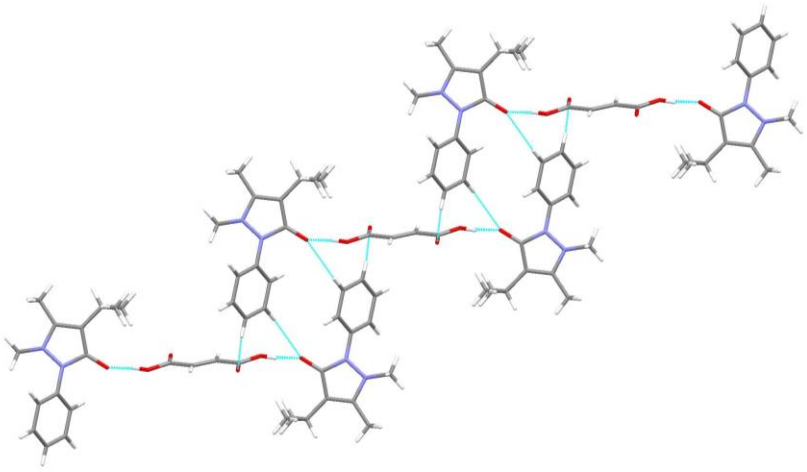

Figure 6. Stepped arrangement of 2:1 PROPY-FA cocrystal containing molecules related by inversion.

PROPY–45DClPA (1:1) cocrystal. The cocrystal comprises a 1:1 stoichiometry with a bifurcated hydrogen bonding pattern of the PROPY carbonyl through both of its lone pairs. These are O–H···O hydrogen bonds (2.58 Å and 2.64 Å, 173° and 177°) from coformer carboxylic acid groups; a single PROPY partakes in hydrogen bonds from two independent coformer molecules and results in a chain (Figure 7). The chains are composed of double layers, where the layers are related by a glide plane to form an alternating motif. These chains stack along the *a*- and *b*-axes.

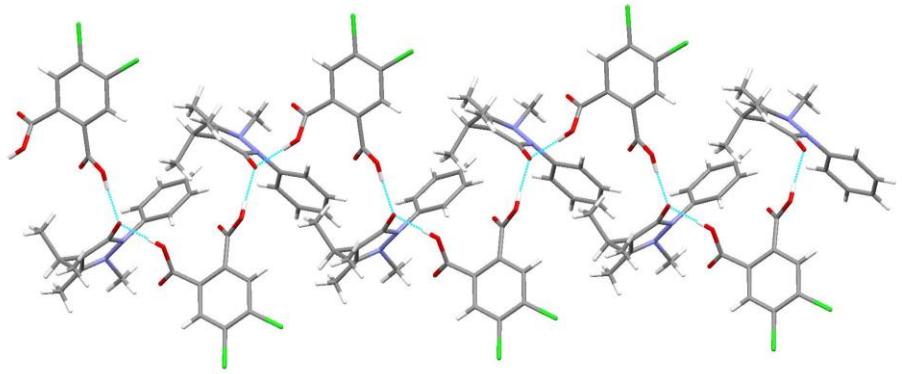

Figure 7. A hydrogen bonded chain in the 1:1 PROPY-45DClPA cocrystal.

Carboxylic Acid and Hydroxyl Functional Groups. Three cocrystals were obtained with coformers containing both a carboxylic acid and at least one hydroxyl functional group, these were with 4-hydroxybenzoic acid (4HBA), 2,5-dihydroxybenzoic acid (25DHBA) and 3,5-dihydroxybenzoic acid (35DHBA).

PROPY–4HBA (1:1) cocrystal. One molecule of each component is present in the asymmetric unit of the PROPY-4HBA cocrystal forming an $O_{hydroxyl}$–H···$O_{carbonyl}$ hydrogen bond (2.673 Å, 178°) and, through a carboxylic acid dimer of two coformers, interact with a second such pair.

These stack to form tapes through C–H···O interactions giving a ladder network consisting of a central coformer dimer and peripheral PROPY molecules (Figure 8). The ladders have two orientations in the crystal lattice, related by 45°, and pack with a square 'box' arrangement.

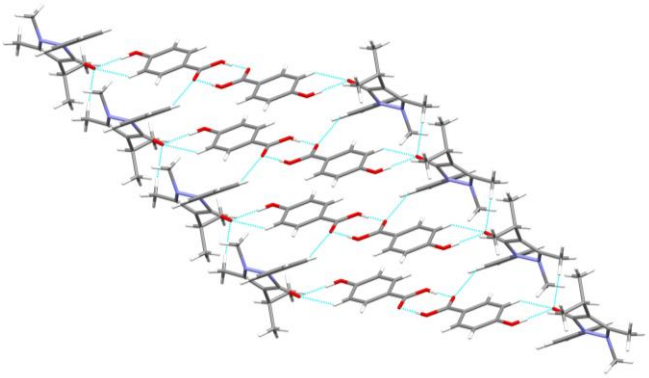

Figure 8. Main interactions in PROPY-4HBA cocrystal (left) and packing viewed down the *a*-axis showing zig-zag construct.

PROPY–35DHBA (1:1) cocrystal. The asymmetric unit of the PROPY-35DHBA cocrystal (Figure 9, top) comprises 4 molecules of each component (see Supporting Information, section 4.3.2 for further information on disorder). The primary interaction is an $O_{hydroxyl}$–H···$O_{carbonyl}$ hydrogen bond, which occurs twice from each coformer molecule to two independent PROPY molecules (2.63-2.74 Å, 171-177°). A carboxylic acid head-to-tail hydrogen bonded dimer is also present. These interactions form a 6-membered motif with central coformer dimer and four surrounding PROPY molecules in opposite orientations on each side of the dimer. A further two coformers form an $O_{hydroxyl}$–H···$O_{carbonyl}$ hydrogen bond with diagonally opposite PROPY molecules in the assembly, i.e. located above and below the dimer on alternate sides. These chains stack in layers parallel to the coformer dimer plane, and interlock perpendicular to this

plane with the additional coformer molecules. A further dimer interaction is seen in these molecules, perpendicular to the original dimer, aiding the packing of these chains and giving a stepped packing arrangement (Figure 9, bottom).

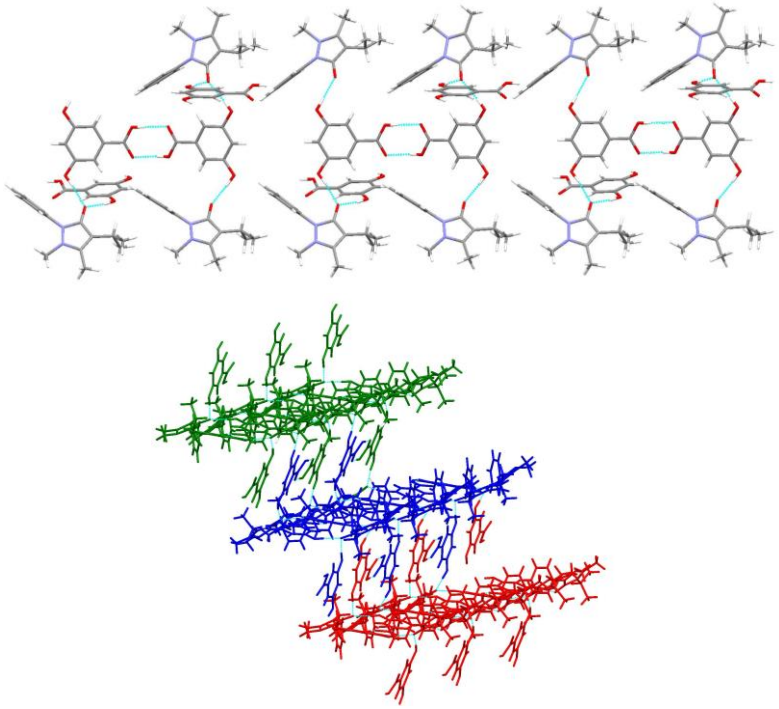

Figure 9. Interactions in the PROPY-35DHBA cocrystal displaying chains of 6-component motifs (top) and interlocking of chains in stepped packing arrangement (below).

PROPY–25DHBA-1,4-dioxane (2:1:1) solvate. Two molecules of PROPY and one molecule each of 25DHBA and 1,4-dioxane constitute the asymmetric unit. The solvent molecules (not displayed) are located in voids and disordered over many positions. Similarly, the coformer also displays disorder over two positions (see Supporting Information, section 4.3.1). The main interactions are an $O_{hydroxyl}$–H···$O_{carbonyl}$ (2.63 Å, 17°) and an O_{acid}–H···$O_{carbonyl}$ (2.55 Å, 164°)

Commented [ML1]: Cif updated and interactions values changed very slightly. These are in agreement with deposited CIF and SI.

hydrogen bond from a single coformer to the two independent PROPY molecules (Figure 10). $C_{isopropyl}$–H···$O_{hydroxyl}$ contacts extend these 2:1 units into staggered chains throughout the lattice.

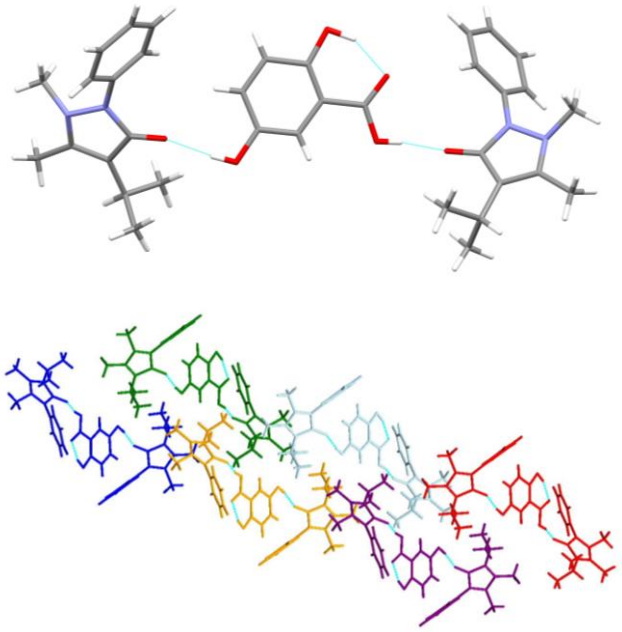

Figure 10. Interactions in the crystal structure of PROPY-25DHBA-1,4-dioxane solvate showing only the major component of the disordered coformer molecule for clarity with no solvent present (above), and chains of staggered 2:1 units (below).

Structural Similarities. The eight new cocrystals contain coformers with hydroxyl and/or carboxylic acid moieties. Three of the coformers contain both a carboxylic acid and hydroxyl group of which all demonstrate an O–H···O hydrogen bond involving hydroxyl and carbonyl groups. Only one of these, the 25DHBA cocrystal, also displays an O–H···O hydrogen bond involving the carboxylic acid of the coformer and carbonyl of PROPY. Of the eight new

cocrystals, five display a bifurcated O–H···O hydrogen bond consisting of coformer OH or CO_2H and an additional coformer C–H contact from the phenyl ring on which the functional group is a substituent.

The cocrystal with FA displays a single O–H···O hydrogen bond involving the PROPY and FA, with additional C-H contacts occurring from PROPY molecules. This is the only structure which contains such an interaction pattern, with multiple PROPY-PROPY contacts. Interestingly, the cocrystals with PGL and 45DClPA coformers display no C–H···O contacts to the carbonyl. Three cocrystals display a ladder network in their crystal structures: those with the coformers 4HBA, 35DHBA and 25DHBA. The ladder in the 35DHBA cocrystal consists of perpendicular 'rungs' however the other structures deviate from a 90° geometry. Two of these (4HBA and 35DHBA cocrystals) display a carboxylic acid dimer of the coformer molecules which is located at the centre of the ladder and may contribute to their similar hydrogen bonding networks.

Crystal structure analysis of the PROPY cocrystals revealed that once the carbonyl is engaged in a hydrogen bond, PROPY does not play a structure directing role due to the lack of hydrogen bond donor functional groups. The coformer hence plays an important role, and the resulting structure is dependent upon the functional groups present on these molecules and the interactions that these form. If there are additional functional groups present, beyond those partaking in interactions with the PROPY molecule, self-interaction can occur and produce different packing motifs (Figuress 4, 5, 7-9). If there are no additional functional groups, as in the case of PROPY-MPAR, space filling then takes precedence in defining the crystal structure(Figure 3). The crystal structures are clearly dependent upon the nature of the differing coformers present,

however all cocrystals exhibit packing coefficients (C_k, Table 1) as expected for organic compounds.[48]

Table 1. Unit cell and molecular volumes, *Z values and packing co*efficents for the eight new cocrystals of PROPY.

Sample	**Z**	**Unit cell volume /Å^3**	**Molecular volume[a] /Å^3**	**C_k[b]**
PROPY-25DHBA, 1,4-dioxane solvate	5	3807.76	670.53 (excluding solvent 583.56)	0.7044 (excluding solvent 0.6130)
PROPY-35DHBA	8	4024.18	355.32	0.7064
PROPY-45DClPA	8	4474.82	393.36	0.7037
PROPY-4HBA	4	1924.05	347.3	0.7220
PROPY-FA	2	757.912	275.27	0.7264
PROPY-HQ	2	1193.76	428.4	0.7177
PROPY-MPAR	4	2031.56	364.83	0.7183
PROPY-PGL, acetonitrile solvate	4	4035.7	718.73	0.7123

[a]Molecular volume calculated using Molinspiration Property Calculation Service (www.molinspiration.com) [b]Kitaigorodsky packing coefficient[48] calculated using the equation: $C_k = Z\ V_{mol} V_{cell}^{-1}$. V_{mol} is the molecular volume (Å^3), V_{cell} is the volume of the unit cell (Å^3), and Z is the number of molecules in the unit cell.

The three coformers which form ladder structures all have similar additional functional groups (CO_2H) hence showing the directing influence on the crystal structure and packing.

Thermal Analysis. All samples were analyzed by Differential Scanning Calorimetry (DSC), Figure 11, which indicates different melting points of the cocrystals compared to that of PROPY.coformer These indicate that the cocrystals can help to improve or modify the stability of PROPY. Of the eight cocrystals reported, three show a lower melting point while the remainder melt at a higher temperature relative to that of pure PROPY. Comparisons to pure coformer melting points can be seen in Table 2. The DSC thermogram of the cocrystal with PGL indicates a number of events, which can be ascribed to loss of solvent (acetonitrile) at 96 °C which may lead to a phase transition (rearrangement upon loss of solvent) at 110 °C with final melt at 117 °C. Further investigation indicated that the recrystallisation event at 143 °C equates to recrystallisation of the coformer, which then melts at 220 °C.

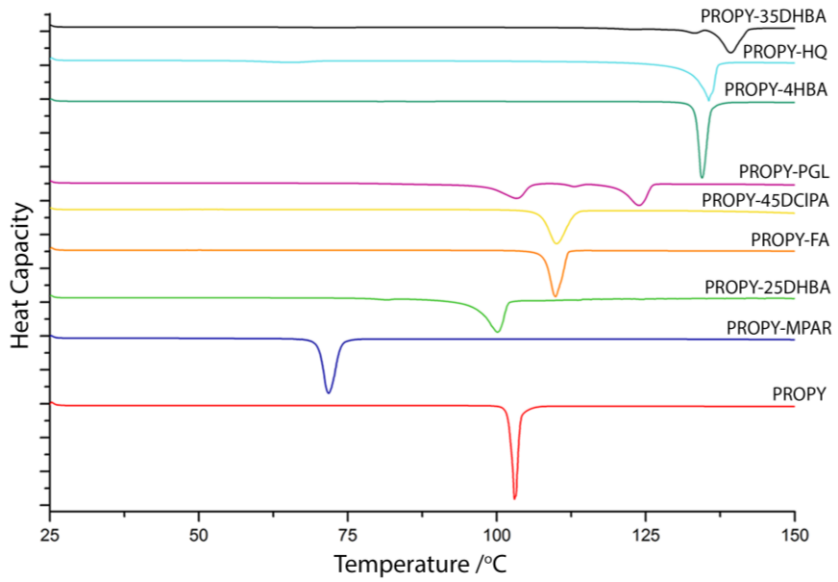

Figure 11. DSC plots for all cocrystals and parent material measured at heating rate of 10°C min^{-1} from 25 °C to 150 °C.

Table 2. Tabulated melting points from DSC experiments alongside reference coformer melting points.

Sample	Cocrystal (API) Melting Point Onset /°C	Co-Former Melting Point /°C
PROPY	102.2	
PROPY-25DHBA	96.4	200-205
PROPY-35DHBA	136.5	236-23
PROPY-45DClPA	107.3	198-200
PROPY-4HBA	133.4	214
PROPY-FA	108.0	287
PROPY-HQ	133.9	172
PROPY-MPAR	70.2	125-128
PROPY-PGL	96.5 / 109.9/ 117.6 recrystallisation event at 143	219

Stability of Cocrystals. Stability of PROPY and cocrystals that contain pharmaceutically acceptable coformers was tested under slurry and accelerated test conditions (40 °C/ 75 % relative humidity). Excess powders of the cocrystals were stirred in pH 7.5 phosphate buffer solution at room temperature. The solids were filtered and air dried after 24 h stirring. The solid samples were analysed by PXRD for assessing the stability of the solids (see Supporting Information, section 5) whilst solution aliquots were diluted appropriately and tested by high-performance liquid chromatography (HPLC) for solubility. Under both sets of conditions, PROPY and all the cocrystals appear stable with the exception of the 25DHBA and PGL systems. This is possibly due to the presence of solvent molecules in the crystal lattice of both samples, particularly in the PROPY-25DHBA cocrystal as the solvent is disordered. After 24

hour slurry both samples show PROPY peaks in the PXRD patterns indicating dissociation. Under accelerated storage conditions, dissociation of the PROPY-25DHBA cocrystal is evident from the appearance of coformer and PROPY peaks in the PXRD patterns however the PROPY-PGL system retains many of the original peaks and shows only a partial dissociation. The PROPY-PGL sample is more stable under these conditions than in an aqueous slurry environment.

Dynamic Vapour Sorption (DVS) measurements were also utilised to determine moisture uptake with an increasing relative humidity over a given time period. Figure 12 shows the sorption and desorption profiles for the five cocrystals with pharmaceutically acceptable coformers and PROPY parent material. All samples with the exception of one, that with PGL as the coformer, display stability even at high relative humidity. The cocrystal with PGL, however, showed a significant mass change indicating water uptake. This structure is a cocrystal solvate, and contains small voids into which water molecules could absorb and hence explain the DVS experiment result.

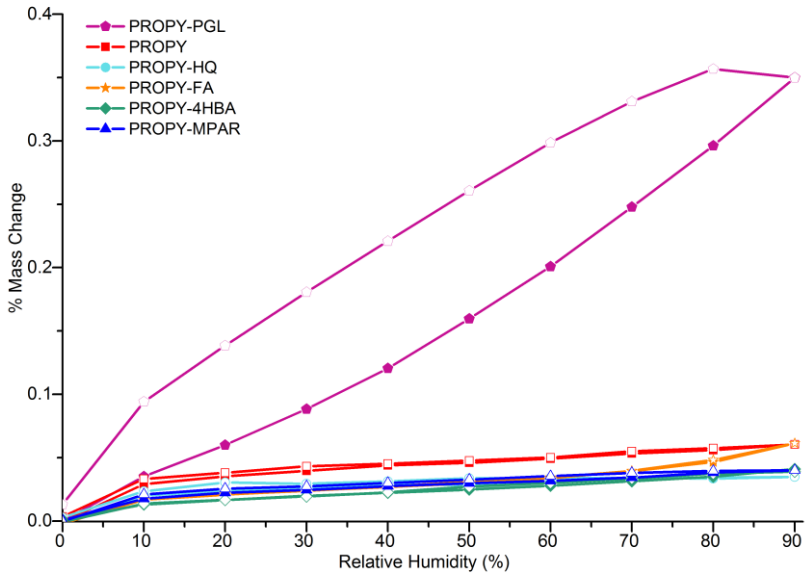

Figure 12. DVS plot of sorption (solid coloured markers) and desorption (hollow markers) of PROPY and cocrystal materials.

Solubility and Dissolution Rate. To optimize drug performance, peak and equilibrium concentrations (kinetic and thermodynamic solubility respectively) of drug are essential in order to understand the substances' behaviour and related drug release. An increase in initial dissolution rate means the drug is released quickly which is advantageous for development of immediate-release drug formulations. Except for the cocrystals with 25DHBA and PGL, all the cocrystals were found to be stable in the slurry experiments therefore the concentration of the aliquots represent the true solubility of the cocrystals. Interestingly, both PROPY-25DHBA and PROPY-PGL are solvate structures which may contribute to their poorer stabilities. The solubility for these samples was calculated according to the literature using the apparent solubility equation (Equation 1).[49, 50]

$$C_m = C_s\left(\frac{J_m}{J_s}\right)$$

Equation 1. Apparent solubility equation where C_m represents the appraent solubility, C_s represents the solubility of the thermodynamic form and J_m and J_s represent the dissolution rates for the co-crystsl and thermodynamic form respectively taken from linear portion of the dissolution profiles.

As shown in Figure 13, all the cocrystals show a significantly higher initial dissolution rate compared to that of PROPY in pH 7.5 phosphate buffer. The dissolution rate of most of the cocrystals reaches a plateau (100% dissolution) within 60 min with HQ system showing the highest dissolution rate, reaching the plateau within 25 min. In contrast the parent PROPY dissolution rate was found to be much slower, only reaching a plateau after 300 min. The solubility data of the cocrystals is compared with the solubility of PROPY in Table 3. The cocrystal with HQ showed the highest solubility of the stable cocrystals followed by the cocrystal with 35DHBA. The solubility of the stable materials follows the trend: PROPY-HQ > PROPY-35DHBA > PROPY > PROPY-4HBA > PROPY-FA > PROPY-MPAR. When compared to the solubilities of the coformers, in general the more soluble coformers result in more soluble cocrystals however the exact trend is not followed. It must be noted that coformer solubilities are reported in water however determined experimentally in a pH 7.5 phosphate buffer and so some discrepencies are to be expected.

The two cocrystals which dissociate in the slurry experiment show higher (apparent) solubilities than those determined from slurry for the stable materials. This is in accordance with many reported studies in which a more soluble cocrystal will eventually produce the less stable API or coformer, ie dissociate.[51] HQ and 35DHBA both produced a cocrystal with an increased

solubility however did not indicate dissociation into component parts (which may be expected of a more soluble cocrystal). This can be rationalised as their solubilities are in the same range as that of PROPY meaning that either parent material or cocrystal may be equally likely to result from a slurry experiment. PROPY-25DHBA and PROPY-PGL both showed significantly higher solubilities hence the less soluble parent components resulted after the slurry experiments.

The dissolution and solubility data is perhaps not as expected with improved dissolution rate not corroborated in the solubility for all materials. This could be attributed to a number of factors, such as kinetics dominating the dissolution rate, influenced largely by coformer solubility, whilst equilibrium solubility is dependent upon thermodynamics and a solution equilibrium of cocrystal, PROPY and coformer. The latter may depend upon relative ratios of the components in solution and the binding constants of complexes in solution. Other factors which may have an impact include the dissolution medium favouring the combinations with specific coformers, particle size, wettability and possible tablet surface recrystallisation affecting drug release.[52-54]

The solubility and dissolution experiments suggest that only one cocrystal (that with HQ) showed an increase in both solubility and dissolution rate and was stable. Other coformers displayed the ability to modify the physiochemical properties however further investigation is required to fully understand the experimental observations made.

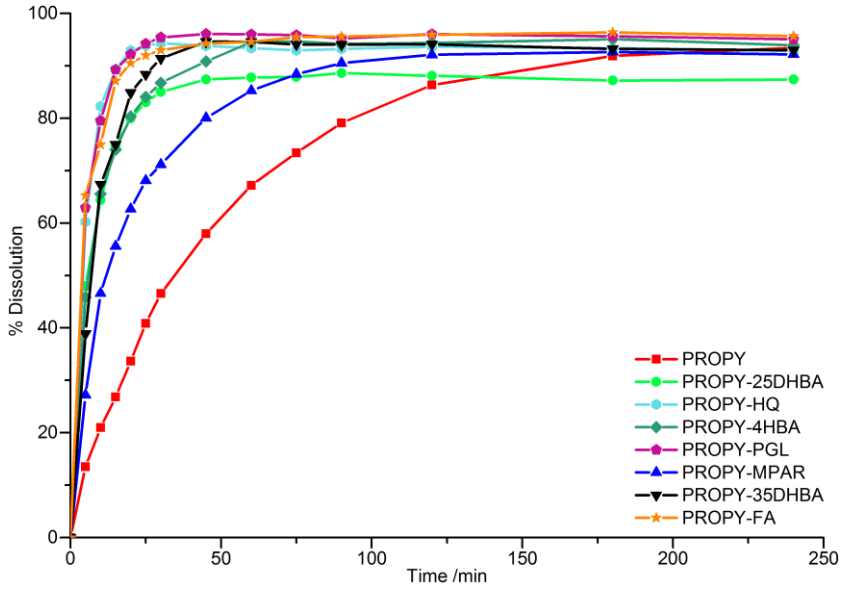

Figure 13. Dissolution profile for PROPY and cocrystals with pharmaceutically acceptable coformers carried out over 240 min experiment time at 37 °C in pH 7.5 phosphate buffer.

Table 3. Solubility of parent API and cocrystals with pharmaceutically acceptable coformers in pH 7.5 phosphate buffer at room temperature.

Sample	Time to reach plateau /min	Solubility /mg mL^{-1}	Ratio to API
PROPY	300	2.71	1
PROPY-4HBA	60	2.19	0.81
PROPY-MPAR	120	1.48	0.55
PROPY-FA	45	1.82	0.67
PROPY-HQ	25	3.14	1.16
PROPY-35DHBA	45	2.76	1.02

PROPY-25DHBA	45	8.49[a]	3.25
PROPY-PGL	30	10.03[a]	3.84

[a] apparent solubility

CONCLUSIONS

Cocrystals in industry are discovered by high throughout screening, often requiring numerous experiments and associated costs. Compounds displaying little or no hydrogen bonding functionality, either through an absence of functional groups, steric hindrance preventing interactions or a combination of the two, pose challenges in coformer prediction and selection for developing multi-component materials. Such systems are not suited to supramolecular synthon design or molecular descriptor-based predictions (primarily based on polarity and heteroatom presence). In particular, for molecules containing only hydrogen bond acceptor groups finding reliable synthons may be more challenging. We have shown that a knowledge-based approach can be applied, and thus focus this screening to the most likely coformers for a target molecule.

Using CSD statistics, combined with other sources of knowledge, we have identified the most likely interactions with PROPY and used this knowledge for coformer selection. Coformers showing great variation in structure containing different functional groups and combinations thereof, as well as no functional groups (to test predictions), were utilised.

There were relatively few structures which display a high degree of similarity to PROPY. Two known systems (edavarone and antipyrine) do not contain similar steric hindrance of the functional group(s) and analysis indicates that NH_2 and CO_2H interactions predominate. When a larger subset was obtained with reduced model specificity these interactions appear to have a lower propensity to form as the subset is not dominated by these specific, highly similar systems.

Eight new cocrystals of PROPY were experimentally observed and characterised by X-ray diffraction techniques and DSC. The successful coformers all contain OH, CO_2H or both these functional groups and form the primary interaction in all crystal structures. The majority of the cocrystals contained a hydroxyl···carbonyl interaction than a carboxylic acid···carbonyl interaction, confirming the findings of the interaction searching. OH functionalities were found to be preferential to CO_2H. Coformers containing both functionalities also confirm this preference as the primary interaction to PROPY is via the hydroxyl. Etter's rules state that carboxylic acid functional groups would preferentially form a homodimer, directing the hydroxyl···carbonyl interaction.[20] This dimer interaction is seen in two of the three structures.

Sterics are a dominant factor in the interaction behaviour of PROPY. The search results indicated NH_2 and NH were likely functional groups to form an interaction (the latter being less favourable) however no cocrystals were obtained with coformers containing either functional group. This may be due to NH_2 being too bulky to access the restricted carbonyl functionality, as well as the environment of the group having a large effect. Other cocrystals may be possible, however are likely to require alternative experimental conditions beyond those attempted.

Physicochemical properties such as stability, solubility, and dissolution rate of those containing pharmaceutically acceptable coformers were measured and it was found that the cocrystal with HQ showed an increase in both solubility and dissolution rate of PROPY.

EXPERIMENTAL METHODS

PROPY was purchased from Tokyo Chemical Industry Co. Ltd, Japan, whilst all coformers were purchased from Sigma Aldrich, Singapore and all used as received without any further

purification. Analytical grade solvents were used for the crystallisation experiments, and HPLC grade for all mobile phase solutions.

Cambridge Structural Database (CSD) Interaction Analysis

Isostar: Interactions between differing descriptions of CO_2H, OH, NH_2 and NH groups (detailed in the Supplementary Information) and a carbonyl group were used in Isostar 2.2.3, 2016[27] for contact searching of generalized functional groups.

Full Interaction Mapping (FIM): The deposited crystal structures for PROPY (refcodes BAQJEK and BAQJEK01) were utilized in the CSD-Materials Suite implemented in Mercury v3.8 build RC2.[28, 30] Probes of alcohol oxygen, water oxygen, uncharged NH nitrogen and RNH_3 nitrogen were used to calculate maps and hotspots to locate the most common areas for such interactions of the carbonyl in PROPY.

Contact Searching:[29] The CSD-Materials Suite in Mercury v3.8 build RC2 was used to define contacts between a selection of OH and NH donor groups and various models of the carbonyl group in PROPY. This returned the number of structures present in the database containing the two groups, and the percentage of times the interaction occurred to give a propensity of interaction formation. Full details of the models and results are available in Supporting Information, section 1.

Screening by grinding. 1:1 Stoichiometric ratios of PROPY and coformer were added to a 10 mL stainless steel grinding jar with 7 mm stainless steel ball and ground for 30 minutes at 20 Hz using a Retsch MixerMill (models MM301 and MM200). Solvent drop grinding experiments had 1 drop of methanol added to the jars prior to grinding. PXRD was used to characterise the materials produced with reference to starting material patterns to identify whether changes were

present, and hence a new cocrystal produced. For a number of combinations, solvent drop grinding resulted in a sticky paste or liquid which could not be characterised by PXRD. In these cases, the experiment was repeated as a dry grind, and if this still resulted in a paste then manual grinding (with much reduced time and force) was implemented. In some instances this was still unsuccessful. Observations were noted and some solution trials attempted.

Single crystal preparation by solution crystallisation. Evaporative methods were used to prepare single crystals of the new materials that were identified as promising from the screening by grinding. These were used in single crystal X-ray diffraction experiments as a well as for characterisation and testing of physicochemical properties.

PROPY-25DHBA cocrystal: PROPY (115.15 mg, 0.5 mmol) and 25DHBA (77.06 mg, 0.5 mmol) were dissolved in 1,4-dioxane (2 mL) at 50 °C then left at ambient conditions for evaporation of solvent to occur. After 1-2 days colourless block crystals were obtained.

PROPY-35DHBA cocrystal: PROPY (115.15 mg, 0.5 mmol) and 35DHBA (77.06 mg, 0.5 mmol) were dissolved in 1,4-dioxane (2 mL) at 50 °C then left at ambient conditions for evaporation of solvent to occur. After 3 weeks, block crystals were formed and the same material also seen to form using ethyl acetate solvent.

PROPY-4HBA cocrystal: PROPY (230.31 mg, 1 mmol) and 4HBA (138.12 mg, 1 mmol) were dissolved in ethyl acetate and acetonitrile solvent mix (2 mL) at 50 °C then left at ambient conditions for evaporation of solvent to occur. After a few days thin plates/needles formed.

PROPY-45DClPA cocrystal: PROPY (115.15 mg, 0.5 mmol) and 45DClPA (117.51 mg, 0.5 mmol) were dissolved in 1,4-dioxane (2 mL) at 50 °C then left at ambient conditions for evaporation of solvent to occur. After a week needle-like crystals formed.

PROPY-FA cocrystal: PROPY (230.31 mg, 1 mmol) and FA (116.08 mg, 0.5 mmol) were dissolved in 1,4-dioxane (2 mL) at 50 °C then left at ambient conditions for evaporation of solvent to occur. After a week colourless blocks and some clusters formed. The cocrystal was also afforded from ethyl acetate-acetonitrile, ethyl acetate-THF and ethyl acetate-1,4-dioxane solvent mixes.

PROPY-HQ cocrystal: PROPY (115.15 mg, 0.5 mmol) and HQ (55.06 mg, 0.5 mmol) were dissolved in 1,4-dioxane (2 mL) at 50 °C then left at ambient conditions for evaporation of solvent to occur. After 2 weeks colourless plates formed. The cocrystal was also afforded from formic acid solvent (crystals forming within a month), and the 1:2 stoichiometry was produced from both 1:1 and 1:2 stoichiometric ratios in solution crystallisation.

PROPY-MPAR cocrystal: PROPY (230.31 mg, 1 mmol) and MPAR (152.15 mg, 1 mmol) were dissolved in an ethyl acetate-acetonitrile solvent mix (2 mL) at 50 °C then left at ambient conditions for evaporation of solvent to occur. After 2 weeks colourless plates formed.

PROPY-PGL cocrystal: PROPY (230.31 mg, 1 mmol) and PGL (126.11 mg, 1 mmol) were dissolved in an ethyl acetate-acetonitrile solvent mix (2 mL) at 50 °C then left at ambient conditions for evaporation of solvent to occur. After a few days colourless plates formed.

Powder X-Ray Diffraction. For powder samples generated from grinding, stability and slurry experiments, PXRD data were collected using a Bruker D8 Advance powder X-ray

diffractometer with Cu-Kα radiation (λ = 1.54060 Å), with 35 kV and 40 mA voltage and current applied. The sample was scanned from 2θ = 5 ° to 50 ° with continuous scan, and a scan rate of 5 °min^{-1}. OriginPro 9.1 was used to plot the PXRD patterns obtained.

Single Crystal X-ray Diffraction. Data for all cocrystals, except PROPY-25DBA, were collected on an Agilent Technologies Dual Source Supernova, four-circle diffractometer fitted with CCD detector and graphite monochromator using Mo-Kα radiation (λ = 0.71073 Å). CrysAlisPro[55] software was used for data collection, reduction and absorption correction using face indexing and Gaussian corrections. PROPY-25DHBA cocrystal data were collected on a Rigaku FRE+ equipped with VHF *Varimax* confocal mirrors, an AFC10 goniometer and an HG Saturn724+ detector using Mo-Kα radiation (λ = 0.71075 Å). Crystal Clear 3.1[56] software was used for data collection and CrysAlisPro for data reduction and Gaussian absorption correction. All data sets were collected at 100 K and suitable crystals selected and mounted using paratone or fomblin oil on a MiTeGen Micromesh holder. Structure solution for all was carried out using Direct Methods in SHELXT[57] and refined using full-matrix least squares on F2 using SHELXL 2014[58] both implemented in the Olex2 software.[59]

Hydrogen atoms for heteroatoms (N and O) were located from the difference Fourier map and all were freely refined. The remaining protons were fixed in idealised positions with their displacement parameters riding on the values of their parent atoms. Non-hydrogen atoms were refined with anisotropic displacement parameters whilst all hydrogen atoms left as isotropic. PLATON,[60] with neutron normalised hydrogen bond lengths (for O–H, N–H and C–H at 0.983 Å, 1.009 Å and 1.008 Å respectively), were used for the calculation of bond lengths and bond angles..

PROPY-25DHBA contains whole molecule disorder of 25DHBA and disordered solvent contained in voids. The solvent masking routine in Olex2 and Platon Squeeze algorithms were implemented and allowed stoichiometry to be determined. PROPY-35DHBA displayed four electron density peaks in the carboxylic acid dimer indicating proton sharing. This was modelled as a 0.5 occupancy hydrogen atom on each oxygen in the dimer arrangement (see Supporting Information, section 4).

CCDC numbers 1504450-1504457 contain the supplementary crystallographic data for this paper and can be obtained from The Cambridge Crystallographic Data Centre via *http://www.ccdc.cam.ac.uk/conts/retrieving.html*.

Crystallographic data, crystal structure information and hydrogen bond parameters for the structures presented can be found in the Supporting Information, section 4.

Differential Scanning Calorimetry (DSC). A TA Instruments Discovery DSC fitted with autosampler and liquid nitrogen pump cooling system was used to measure the thermal behaviour of all samples. Dried samples (free from residual solvent), of mass 2-5 mg, were placed in an aluminum pan (internal volume 20 μL) and crimp sealed with corresponding lid in a Tzero sample press. The heating range was set as 25 °C to 150 °C, with a heating rate of 10 °C min^{-1} and nitrogen gas used for purging (base purge 300 mL min^{-1}).

Stability Studies. Stability of PROPY and all the cocrystals except 45DCIPA (not pharmaceutically acceptable) was tested using storage under accelerated conditions (40 °C and 75 % relative humidity) for 13-15 weeks. Samples of approximately 100 mg size were stored under the test conditions and tested periodically using PXRD to identify the sample's identity.

For slurry experiments, excess cocrystal materials in pH 7.5 phosphate buffer solution were left stirring at room temperature for 24 hours before filtering and the resulting powder analysed by PXRD. Solubility of the samples was measured by taking aliquots of the filtered slurry solution and analyzing by HPLC.

Dynamic Vapour Sorption (DVS). DVS analysis was carried out on a Surface Measurement Systems DVS Advantage machine. A preheating stage, raising the temperature to 40 °C with an isothermal hold for 5 hours, was followed by increasing the partial pressure at 0.2 % per minute from 0-90 % relative humidity.

Dissolution Rate. Dissolution rate was tested using sink conditions for five pharmaceutically acceptable cocrystals and parent material using an Agilent 708-DS dissolution sampling apparatus with rotation speed of 75 rpm at 37 °C. Phosphate buffer solution (pH 7.5) was used as the dissolution medium (900 mL) with samples prepared containing 75 mg API in a 500 mg cornstarch tablet, pressed for 1 minute at 2 KN using an FT-IR press. Sampling was conducted by withdrawing 2 mL of sample from the vessel and immediately replaced with fresh dissolution medium to maintain the dissolution volume. 1 mL was discarded as waste and a sample taken for analysis by HPLC after filtering through a 45 μm syringe tip filter. This was conducted at 5 minute intervals for the first 30 minutes followed by 15 minutes for 30 minutes, a 120 minute sample taken and then hourly to the end of the experiment.

Apparent solubility calculations were determined as indicated in the literature,[49, 50] using the linear portions of the dissolution curves for PROPY (0-30 mins, R^2 0.9815), PROPY-25DHBA (0-15 mins, R^2 0.8823) and PROPY-PGL (0-15 mins, R^2 0.8374).

High Performance Liquid Chromatography (HPLC). HPLC analysis was carried out to quantitatively determine PROPY concentration by using a HP 1100 pump fitted with G1315B (Agilent Technologies) diode array detector. The LC column was an Agilent Lichrosorp-RP-18, dimensions 4.6 x 200 mm, 5 µm run at 37 °C. The mobile phase consisted of acetonitrile and water (50:50 v/v) which was filtered through a 45 µm cellulose filter membrane under vacuum and then sonicated. The mobile phase was pumped isocratically at a flow rate of 1.5 mL min^{-1} with a 12 minute run time. An injection volume of 10 µL was used and detection wavelength for all analytes was 280 nm. Retention times were: PROPY 4.29 mins, 35DHBA 0.93 mins, FA 1.05 mins, 4HBA 1.18 mins, HQ 1.73 mins and MPAR 2.32 mins. This method was created using information from the work by David *et al*.[61]

ASSOCIATED CONTENT

Supporting Information.

Details of CSD searches, coformers, PXRD patterns from grinding, slurry and accelerated stability tests, crystal structure parameters and hydrogen bonding tables can be found in the Supporting Information, and is available free of charge on the ACS publications website http://pubs.acs.org. CIF files for all crystal structures are deposited in the CSD, CCDC numbers 1504450-1504457.

AUTHOR INFORMATION

Corresponding Author

*Email: srinivasulu_aitipamula@ices.a-star.edu.sg

Notes

The authors declare no competing financial interest.

ACKNOWLEDGMENTS

This research was funded by the Science and Engineering Research Council of A*STAR (Agency for Science, Technology and Research), Singapore. Lucy Mapp thanks A*STAR for a research fellowship jointly funded by the A*STAR Research Attachment Programme (ARAP) and The University of Southampton.

REFERENCES

(1) Childs, S. L.; Zaworotko, M. J., *Cryst. Growth Des.* **2009,** *9*, 4208-4211.
(2) Aitipamula, S.; Banerjee, R.; Bansal, A. K.; Biradha, K.; Cheney, M. L.; Choudhury, A. R.; Desiraju, G. R.; Dikundwar, A. G.; Dubey, R.; Duggirala, N.; Ghogale, P. P.; Ghosh, S.; Goswami, P. K.; Goud, N. R.; Jetti, R. R. K. R.; Karpinski, P.; Kaushik, P.; Kumar, D.; Kumar, V.; Moulton, B.; Mukherjee, A.; Mukherjee, G.; Myerson, A. S.; Puri, V.; Ramanan, A.; Rajamannar, T.; Reddy, C. M.; Rodriguez-Hornedo, N.; Rogers, R. D.; Row, T. N. G.; Sanphui, P.; Shan, N.; Shete, G.; Singh, A.; Sun, C. C.; Swift, J. A.; Thaimattam, R.; Thakur, T. S.; Kumar Thaper, R.; Thomas, S. P.; Tothadi, S.; Vangala, V. R.; Variankaval, N.; Vishweshwar, P.; Weyna, D. R.; Zaworotko, M. J., *Cryst. Growth Des.* **2012,** *12*, 2147-2152.
(3) Thakuria, R.; Delori, A.; Jones, W.; Lipert, M. P.; Roy, L.; Rodriguez-Hornedo, N., *Int. J. Pharm. (Amsterdam, Neth.)* **2013,** *453*, 101-125.
(4) Schultheiss, N.; Newman, A., *Cryst. Growth Des.* **2009,** *9*, 2950-2967.
(5) Duggirala, N. K.; Perry, M. L.; Almarsson, Ö.; Zaworotko, M. J., *Chem. Commun.* **2016,** *52*, 640-655.
(6) Blagden, N.; Coles, S. J.; Berry, D. J., *CrystEngComm* **2014,** *16*, 5753-5761.
(7) Qiao, N.; Li, M.; Schlindwein, W.; Malek, N.; Davies, A.; Trappitt, G., *International journal of pharmaceutics* **2011,** *419*, 1-11.
(8) Steed, J. W., *Trends in pharmacological sciences* **2013,** *34*, 185-93.
(9) Bolla, G.; Nangia, A., *Chemical Communications* **2016,** *52*, 8342-60.
(10) Stanton, M. K.; Bak, A., *Cryst. Growth Des.* **2008,** *8*, 3856-3862.
(11) Babu, N. J.; Nangia, A., *Cryst. Growth Des.* **2011,** *11*, 2662-2679.
(12) Gao, Y.; Zu, H.; Zhang, J., *J. Pharm. Pharmacol.* **2011,** *63*, 483-490.
(13) Aitipamula, S.; Chow, P. S.; Tan, R. B. H., *CrystEngComm* **2014,** *16*, 3451-3465.
(14) Shan, N.; Perry, M. L.; Weyna, D. R.; Zaworotko, M. J., *Expert Opin. Drug Metab. Toxicol.* **2014,** *10*, 1255-1271.
(15) Wood, P. A.; Feeder, N.; Furlow, M.; Galek, P. T. A.; Groom, C. R.; Pidcock, E., *CrystEngComm* **2014,** *16*, 5839-5848.
(16) Desiraju, G. R., *Angew. Chem., Int. Ed.*. **1995,** *34*, 2311-2327.
(17) Cheney, M. L.; Weyna, D. R.; Shan, N.; Hanna, M.; Wojtas, L.; Zaworotko, M. J., *Cryst. Growth Des.* **2010,** *10*, 4401-4413.

(18) Mir, N. A.; Dubey, R.; Desiraju, G. R., *IUCrJ* **2016,** *3*, 96-101.
(19) Ghosh, S.; Bag, P. P.; Reddy, C. M., *Cryst. Growth Des.* **2011,** *11*, 3489-3503.
(20) Etter, M. C., *Acc. Chem. Res.* **1990,** *23*, 120-126.
(21) Etter, M. C.; Frankenbach, G. M., *Chem. Mater.* **1989,** *1*, 10-12.
(22) Aitipamula, S.; Vangala, V. R.; Chow, P. S.; Tan, R. B. H., *Cryst. Growth Des.* **2012,** *12*, 5858-5863.
(23) Takata, N.; Takano, R.; Uekusa, H.; Hayashi, Y.; Terada, K., *Cryst. Growth Des.* **2010,** *10*, 2116-2122.
(24) Karki, S.; Friščić, T.; Fábián, L.; Jones, W., *CrystEngComm* **2010,** *12*, 4038-4041.
(25) Fábián, L., *Cryst. Growth Des.* **2009,** *9*, 1436-1443.
(26) Allen, F., *Acta Crystallogr. B* **2002,** *58*, 380-388.
(27) Bruno, I.; Cole, J.; Lommerse, J. M.; Rowland, R. S.; Taylor, R.; Verdonk, M., *J. Comput. Aided Mol. Des.* **1997,** *11*, 525-537.
(28) Bruno, I. J.; Cole, J. C.; Edgington, P. R.; Kessler, M.; Macrae, C. F.; McCabe, P.; Pearson, J.; Taylor, R., *Acta Crystallogr. B* **2002,** *58*, 389-397.
(29) Macrae, C. F.; Bruno, I. J.; Chisholm, J. A.; Edgington, P. R.; McCabe, P.; Pidcock, E.; Rodriguez-Monge, L.; Taylor, R.; van de Streek, J.; Wood, P. A., *J. Appl. Crystallogr.* **2008,** *41*, 466-470.
(30) Macrae, C. F.; Edgington, P. R.; McCabe, P.; Pidcock, E.; Shields, G. P.; Taylor, R.; Towler, M.; van de Streek, J., *J. Appl. Crystallogr.* **2006,** *39*, 453-457.
(31) Kiersch, T. A.; Minic, M. R., *Curr Med Res Opin* **2002,** *18*, 18-25.
(32) Müller, B. W.; Beer, Y., *Acta Pharm. Technol.* **1982,** *28*, 97-102.
(33) Lemmerer, A.; Bernstein, J.; Griesser, U. J.; Kahlenberg, V.; Többens, D. M.; Lapidus, S. H.; Stephens, P. W.; Esterhuysen, C., *Chemistry – A European Journal* **2011,** *17*, 13445-13460.
(34) Zalac, S.; Khan, M. Z.; Gabelica, V.; Tudja, M.; Mestrović, E.; Romih, M., *Chem. Pharm. Bull* **1999**, 302-7.
(35) Dörler, G. PhD Thesis. University of Innsbruck (Austria), 1982.
(36) Alberola, A.; Rambaud, J.; Sabon, F., *Ann. Pharm. Fr.* **1972,** *34*, 95-99.
(37) Alberola, S.; Sabon, F.; J.Jaud; Galy, J., *Acta Cryst* **1977,** *B33*, 3337-3341.
(38) Rambaud, J.; Jeanjean, B.; Pauvert, B.; Alberola, S., *Bull. Soc. Chim. Fr.* **1986**, 620-624.
(39) Issa, N.; Barnett, S. A.; Mohamed, S.; Braun, D. E.; Copley, R. C. B.; Tocher, D. A.; Price, S. L., *CrystEngComm* **2012,** *14*, 2454-2464.
(40) Singh, T. P.; Vijayan, M., *Acta. Cryst. Sect. B: Struct. Crystallogr. Cryst. Chem.* **1974,** *B30*, 557-562.
(41) Lyczko, K., *Acta Crystallogr. Sect. Sect. E: Struct. Rep. Online* **2013,** *69*, o127-o128.
(42) Tordjman, I.; Durif, A.; Masse, R., *Acta Crystallogr. Sect. C: Cryst. Struct. Commun.* **1991,** *47*, 351-353.
(43) Veverka, M.; Dubaj, T.; Gallovič, J.; Švajdlenka, E.; Meľuchová, B.; Jorík, V.; Šimon, P., *Monatshefte für Chemie - Chemical Monthly* **2013,** *144*, 1335-1349.
(44) Trask, A. V.; Motherwell, W. D. S.; Jones, W., *Chem. Commun.* **2004**, 890-891.
(45) James, S. L.; Adams, C. J.; Bolm, C.; Braga, D.; Collier, P.; Friscic, T.; Grepioni, F.; Harris, K. D. M.; Hyett, G.; Jones, W.; Krebs, A.; Mack, J.; Maini, L.; Orpen, A. G.; Parkin, I. P.; Shearouse, W. C.; Steed, J. W.; Waddell, D. C., *Chem. Soc. Rev.* **2012,** *41*, 413-447.
(46) Trask, A. V.; Jones, W., *Top. Curr. Chem.* **2005,** *254*, 41-70.

(47) ChemAxon *MarvinSketch 16.4.25*, 2016.
(48) Kitaigorodski, A. I., *Organic Chemical Crystallography*. ed.; Consultants Bureau: New York, 1961.
(49) Fagerberg, J. H.; Tsinman, O.; Sun, N.; Tsinman, K.; Avdeef, A.; Bergström, C. A. S., *Mol. Pharmaceut.* **2010,** *7*, 1419-1430.
(50) Sanphui, P.; Goud, N. R.; Khandavilli, U. B. R.; Nangia, A., *Cryst. Growth Des.* **2011,** *11*, 4135-4145.
(51) Reddy, L. S.; Bethune, S. J.; Kampf, J. W.; Rodríguez-Hornedo, N. r., *Cryst. Growth Des.* **2008,** *9*, 378-385.
(52) Blagden, N.; Berry, D. J.; Parkin, A.; Javed, H.; Ibrahim, A.; Gavan, P. T.; De Matos, L. L.; Seaton, C. C., *New J. Chem.* **2008,** *32*, 1659-1672.
(53) Blagden, N.; de Matas, M.; Gavan, P. T.; York, P., *Adv. Drug Deliv. Rev.* **2007,** *59*, 617-630.
(54) Aaltonen, J.; Rades, T., *Dissolut. Technol* **2009,** *16*, 47-54.
(55) *CrysalisPro*, Agilent Technologies: Oxfordshire, 2013.
(56) *CrystalClear*, Rigaku Corporation: Tokyo, Japan, 2009.
(57) Sheldrick, G., *Acta Crystallographica Section A Foundations and Advances* **2015,** *71*, 3-8.
(58) Sheldrick, G. M., *Acta Crystallogr.* **2008,** *A64*, 112-122.
(59) Dolomanov, O. V.; Bourhis, L. J.; Gildea, R. J.; Howard, J. A. K.; Puschmann, H., *J. Appl. Crystallogr.* **2009,** *42*, 339-341.
(60) Spek, A., *Acta Crystallographica Section D* **2009,** *65*, 148-155.
(61) Soponar, F.; Staniloae, D.; Moise, G.; Szaniszlo, B.; David, V., *Rev. Roum. Chim.* **2013,** *58*, 433-440.

For Table Of Contents Use Only

Design of Cocrystals for Molecules with Limited Hydrogen Bonding Functionalities:

Propyphenazone as a Model System

Lucy K. Mapp,[†,‡] Simon J. Coles,[‡] Srinivasulu Aitipamula*[,†]

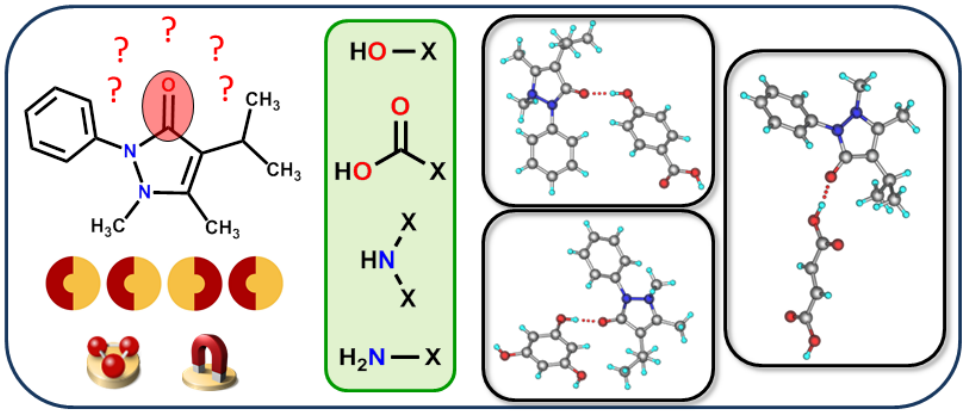

Propyphenazone possesses limited or no hydrogen bonding functionality and, along with other similar molecules, present difficulties in selection of coformers for cocrystal design. A knowledge-based strategy was used to identify appropriate coformers and eight new cocrystals resulted and characterized by X-ray diffraction techniques. Evaluation of physiochemical properties of cocrystals revealed comparable stability to propyphenazone and a cocrystal with hydroquinone improved the solubility and dissolution rate of propyphenazone.